

Laboratory comparison of evaporation rate between Colorado Sanken evaporation pan and Class A evaporation pan (Case study: Semnan, Iran)

Hamidreza Ghazvinian¹, Hojat Karami^{2*}, Changhyun Jun^{3*}, Oceana Francis⁴, Sayed M. Bateni⁵, Yashar Dadras-Ajirlou⁶, Shahab S. Band^{7*}

¹ Civil Engineering Department, Semnan University. Email: (Hamidrezaghazvinian@semnan.ac.ir)

² Civil Engineering Department, Semnan University. Email (hkarami@semnan.ac.ir)

³ Department of Civil and Environmental Engineering, College of Engineering, Chung-Ang University, Seoul 06974, Korea; E-mail: cjun@cau.ac.kr

⁴ Department of Civil and Environmental Engineering and Water Resources Research Center, University of Hawaii at Manoa, Honolulu, HI, USA; E-mail: oceanaf@hawaii.edu

⁵ Department of Civil and Environmental Engineering and Sea Grant College Program, University of Hawaii at Manoa, Honolulu, HI, USA; E-mail: smbateni@hawaii.edu

⁶ Civil Engineering Department, Semnan University. Email: (Dadras_yashar@semnan.ac.ir)

⁷ Future Technology Research Center, College of Future, National Yunlin University of Science and Technology, 123 University Road, Yunlin 64002, Taiwan, (shahab@yuntech.edu.tw)

Abstract: One method of estimating the evaporation rate (ER) is to use a variety of evaporation pans, such as the Class A standard evaporation pan (CASEP) and the Colorado Sanken standard evaporation pan (CSSEP). In this study, the rate of evaporation of CASEP and CSSEP have been investigated and compared with each other. This study was conducted in Semnan, Iran. CSSEP was used as a test pan, which was performed in an open space around the Faculty of Civil Engineering, Semnan University. Evaporation was recorded daily for 123 days. The evaporation of the CASEP pan was obtained from the synoptic station of Semnan, which is located at a distance of 2.39 km from the test site. Meteorological data were also obtained from the synoptic station of Semnan and compared with experimental evaporation data. The results of this study showed that the daily ER from CASEP and CSSEP in the tested time periods were not significantly different. Based on the Klotz-Sminrov method, the best statistical distributions for CASEP and CSSEP were calculated as Error and Gamma, respectively. The coefficient of determination (R^2) between the two pans was estimated to be about 93%. Also, by examining the ER with other meteorological data, it was observed that the ER has the highest correlation with the average daily air temperature.

Keywords: Evaporation; Class A standard evaporation pan; Colorado Sanken standard evaporation pan; Semnan

1-. Introduction

In many hot and dry areas, large volumes of water stored behind dams, agricultural ponds, and water storage tanks are wasted by evaporation (Torres and Calera, 2010). Evaporation plays an important role in the management of water resources, climate change and agriculture (Wang et al., 2017; Ghazvinian et al., 2020b, 2020c). Given the global climate change, researchers have conducted many studies on evaporation worldwide and its evaluation for identification in the hydrological cycle (Miralles et al., 2015). The development of methods for calculating evaporation from water storage ponds, dam reservoirs and even lakes has been of interest to researchers in recent decades, due to the complexity of its nature and measurement as an important challenge has been raised (McMahon et al., 2013). Accuracy in estimating the rate of evaporation in global environmental change research programs, watershed management in basins, as well as in sustainable agricultural development (Jia et al., 2012) is important. Therefore, evaporation of reservoirs, lakes and pools is very effective in water management (Wurbs and Ayala, 2014).

Evaporation and its estimation have many applications in engineering sciences, hydrology, agriculture, and other studies. Numerous studies have been conducted to estimate different evaporation methods (Piri et al., 2009; Guven and Kişi, 2011; Nourani and Sayyah Fard, 2012; Malik and Kumar, 2015; Ghorbani et al., 2018; Alsumaiei, 2020; Ashrafzadeh et al., 2020; Patle et al., 2020). One of the most common methods for measuring evaporation is the use of an evaporation pan (Epan) (Ghazvinian et al., 2020d; Karami et al., 2021), which is used in many different organizations (Stanhill, 2002). Numerous studies have also been conducted to compare evaporation field measurements.

Jia-lian et al. (1996) placed evaporation pans in the soil and exposed the pans to the air at Lake Nancy Station to investigate the rate of evaporation. The results showed that buried devices (such as E601 and GGI-3000) had a higher ER than devices that were exposed to air (such as CASEP and $\phi 20$). Another study includes Fu et al. (2004) who compared 15 types of evaporators with an evaporation tank of 20 square meters and found that the values of the correction coefficient for the evaporation pan $\phi 20$ could be changed by 0.6 and for the evaporation pan E601B by 1.07.

Masoner et al. (2008) compared the ER in a floating evaporation pan with the ER in a CASEP. The results showed that the use of a floating evaporation pan could have a better simulator for estimating water surface evaporation than a CASEP.

Liu et al., (2009) compared the rate of pan evaporation and actual evaporation with the Land surface model in the Xinjing region of China from 1960 to 2005. By examining climatic parameters, pan evaporation and actual evaporation can complement each other. Also, the results from the evaporation pan and the real evaporation have a high correlation with daily temperature, wind speed and relative humidity, which is in line with the results of several research studies (Moghaddamnia et al., 2009; Traore et al., 2010, 2016; Nourani and Sayyah Fard, 2012; Simba and Matorevhu, 2013; Wang et al., 2017).

Chu et al. (2016) compared two CASEPs, one in completely standard condition with a galvanized main color and the other with white. All meteorological parameters were the same for the two pans. The results of this study showed that the ER in the white CASEP was 75% of the standard evaporation pan. Another study by Li et al. (2016) compared two types of evaporation pans in eight regions in China using the coefficient of determination (R^2). They also studied the spatial distribution and conversion ratio of the pans in the target areas. The studied pans were E601B and $\phi 20$, which are commonly used in meteorological stations in China. The results showed that, in the warm seasons of the year, the Kp values in the southwestern regions are higher than one and the Kp values in the northeastern regions are less than one, while in general, the Kp values in the warm seasons are less than the cold seasons. In addition, pure radiation is the predominant climatic factor affecting Kp changes, relative humidity, and lack of vapor pressure.

Ghazvinian et al. (2020b) investigated and compared evaporation from CSSEP and CSSEP containing MDF sheets. The results showed that the ER from the MDF-containing pan was 91% lower than that of the CSSEP. Ghazvinian et al. (2021) went on to place various coatings such as polystyrene, wood, and synthetic honey wax on the CSSEP, where they measured the evaporation and compared the ER from the control pan with the pan containing the coatings. The results showed that the rate of evaporation in the pan containing polystyrene was less than the evaporation in other pans and the control pan.

According to these studies that have been done in the field using different methods of estimating evaporation and comparing these methods, in our study we try to compare the evaporation data of two standard CASEP and CSSEP, which are the most common pans used to measure the rate of evaporation in the world.

The present study examines the following:

1. Present a method for achieving the daily ER using the CSSEP.
2. Compare the ER measured by the CSSEP with the CASEP of a nearby synoptic station.
3. Review of factors, such as: temperature, wind speed, sunlight hours, air pressure and relative humidity on evaporation, that have been studied.

4. Show how the amount of evaporation in the CSSEP that has been tested is different from the CASEP of the synoptic station and whether is there a significant difference between the two pans.

2-. Materials and methods

2-1. Study place

Evaporation was measured in the city of Semnan, which is located in the northeast of Iran. Evaporation measurement for the CSSEP was performed on the north side of the Faculty of Civil Engineering, Semnan University and in a completely open space behind the faculty building. The geographical information of the Faculty of Civil Engineering is equal to a longitude of 53 degrees and 26 minutes east and the latitude of 35 degrees and 36 minutes north and a height of 1149 meters above mean sea level.

The CSAEP data was obtained from the Semnan Synoptic Station, which is the closest station to the test site (2.39 km from the test site). The Semnan Synoptic Station has a longitude of 53 degrees and 25 minutes and a latitude of 35 degrees and 36 minutes and a height of 1127 meters above mean sea level. Also, all data such as temperature (T), wind speed (WS), sunlight hours (SH), air pressure (PA) and relative humidity (RH) were obtained from the Semnan synoptic station (Dehghanipour et al., 2021). Figure 1 shows a map of the studied area.

In order to classify the synoptic station of Semnan city, the Dumarten method was used and according to this method, the value of the drought index was calculated using Equation 1.

$$I = \frac{P}{T + 10}$$

(1)

In the above relation, Equation 1, P represents the average annual rainfall in millimeters, T represents the average annual temperature in degrees Celsius and I represents the drought coefficient (Dumarten coefficient). Based on Equation 1 and Table 1, the Dumarton method divides the regions into six groups: dry, semi-arid, Mediterranean, semi-humid, wet and very humid. According to the observational data in the studied synoptic station and using Domarten method, the type of climate in Semnan is dry.

Table 1: Climatic classification based on the Dumarten method.

Climate name	Domarton drought coefficient range
Dry	Less than 10
Semi-Dry	10 to 19.9
Mediterranean	20 to 23.9
Semi-wet	24 to 27.9
wet	28 to 34.9
Very wet	More than 35

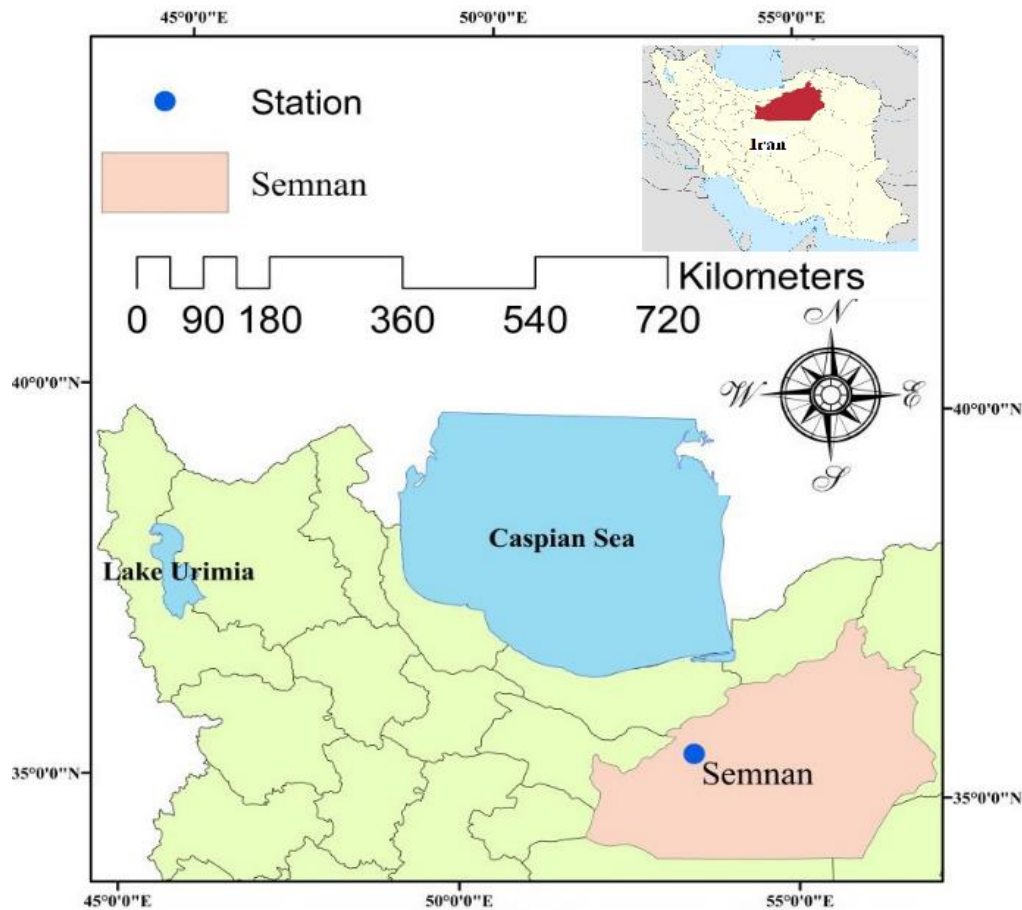


Figure 1: Aerial photo of Semnan research area and synoptic station.

2.2. Evaporation pans under study

Evaporation pans come in a variety of shapes and sizes. CASEP is one of the most common pans (Karamouz et al., 2012; Alsumaiei, 2020). This evaporation pan is made of galvanized iron and has a diameter of 4 feet (120.7 cm) and a depth of 10 inches (25 cm). The pan is placed on a wooden plate (Chu et al., 2010). Other standard evaporation pans include CSSEP (Brutsaert, 1982). The CSSEP is square, 3 feet (92 cm) long and 18 inches (46 cm) deep. This pan is made of 3 mm thick iron and is placed in the soil in such a way that its edge is located at a distance of 2 inches (5 cm) above the soil surface (Kohler, 1954). The outer surface of the pan is covered with bitumen. The water of the pan is kept at or slightly below the soil surface, i.e. at a height of 5 to 5.7 cm from the edge of the pan (Subramanya, 2013). Figure 2 shows a CASEP and a CSSEP.



Figure 2: Dimensions of the studied pans, a) CSSEP and b) CASEP.

2-3. Steps of testing

The tests of this research were performed from May 23, 2018 to September 22, 2018 for 4 months. Data related to CSSEP were read daily at the same time as the CASEP of Semnan Synoptic Station. The readings were read simultaneously at 10:30 a.m. local time and daily. According to the manufacture's specifications, the CSSEP (Subramanya, 2013) is made of galvanized stainless steel.

Figure 3 shows the CSSEP that was built for testing. To increase the accuracy of the test, three CSSEPs were constructed, which are the three test treatments. As mentioned, CASEP data were also received daily for analysis and compared with the SCCEP. Figure 4 shows the CASEP in the Semnan Synoptic Station.



Figure 3: CSSEP made for testing.



Figure 4: CASEP of the Semnan synoptic station.

Evaporation data for the CSSEP and CASEP are from May 23, 2018 to September 22, 2018. The reason for conducting this field study and measuring the evaporation, during these days, is that the rate of evaporation is high at the end of spring and summer.

The city of Semnan is a hot and dry region, so the rainy days during the test period were limited to June 3, June 12, August 8, September 19 and September 20, with a rainfall of 1/3, 2.2, 0.1, 0.3 and 1 mm, respectively. These five rainfall events are considered in the evaporation measurements.

2-4. Statistical analysis

For statistical analysis, after recording the measurement results of the coating data, the ER values were analyzed using SPSS21 software. Statistical correlation between dependent variable and independent variable was analyzed using Pearson bivariate correlation. The Pearson test is used when the levels of measurement of both independent and dependent variables are distant or quantitative. In this study, the correlation between minimum temperature, maximum temperature, minimum humidity, maximum humidity, pressure, sunlight, wind speed and data of the CASEP and CSSEP was investigated. Figure 5 shows a histogram of the data for the CASEP and CSSEP.

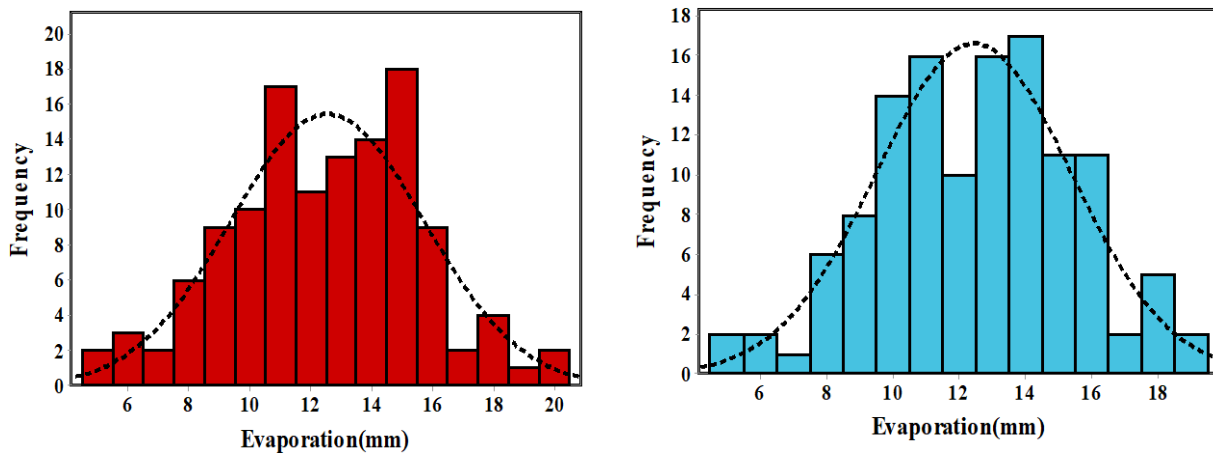


Figure 5: Evaporation data histogram a) CSSEP (left panel, red) and b) CASEP (right panel, blue).

2-5. HEC-SSP

HEC-SSP software, in 2008, was presented by U.S. Army Corps of Engineers for statistical analysis of hydrological data (Brunner and Fleming, 2010). This software has different parts such as data definition and analysis (Harris et al., 2008; Root and Papakos, 2010). In the present study, in the data definition section, the evaporation data of the CSSEP and CASEP were entered. Then, in the Distribution Fitting Analysis section, different statistical distributions were fitted to the data. As a result, the best distribution was selected.

The Kolmogorov-Smirnov test is then used to measure the adherence of samples to a specific distribution (Massey Jr, 1951; Wilks, 1995; Simolo et al., 2010).

The statistics of this test is the largest difference between the expected and actual frequencies (as an absolute value) measured in different categories (Equation 2). Table 2 presents the parameters and relationships of the superior distributions examined in the Results section.

$$D_n(x) = \max |F_n(x) - S_n(x)| \quad (2)$$

$F_n(x)$ is the actual cumulative relative frequency and $S_n(x)$ is the expected cumulative relative frequency (Jahan et al., 2019).

Table 2: Statistical distributions

Distribution	Formulas	Parameters
Error	$f(x) = c_1 \sigma^{-1} \exp \left[- \left c_0^{1/2} \sigma^{-1} (x - \mu) \right ^\nu \right]$	$\text{where } c_0 = \frac{\Gamma\left(\frac{3}{\nu}\right)}{\Gamma\left(\frac{1}{\nu}\right)} \text{ and } c_1 = \frac{\nu c_0^{1/2}}{2\Gamma\left(\frac{1}{\nu}\right)}$ $\mu \in \text{Mean}$ $\sigma^2 \geq 0 = \text{Variance}$ $\nu > 0$
Pearson 6	$f(x) = \frac{1}{\beta B(\alpha_1, \alpha_2)} \frac{(x/\beta)^{\alpha_1-1}}{\left(1 + \frac{x}{\beta}\right)^{\alpha_1+\alpha_2}}$	$\text{where } B(\alpha_1, \alpha_2) \text{ is a Beta function}$ $\alpha_1 > 0, \alpha_2 > 0, \beta > 0$
Log normal	$f(x) = \frac{1}{x \sigma \sqrt{2\pi}} \exp \left(-\frac{(\ln x - \mu)^2}{2\sigma^2} \right)$	$\mu \in \text{Mean}$ $\sigma^2 \geq 0 = \text{Variance}$
Weibull	$f(x) = \alpha \beta^{-\alpha} x^{\alpha-1} \exp \left[-\left(\frac{x}{\beta}\right)^\alpha \right]$	$\alpha > 0, \beta > 0$
Kumaraswamy	$f(x) = \alpha \beta x^{\alpha-1} (1 - x^\alpha)^{\beta-1}$	$\alpha > 0, \beta > 0$
Gamma	$f(x) = \frac{\beta^{-\alpha} x^{\alpha-1} \exp \left(-\frac{x}{\beta} \right)}{\Gamma(\alpha)}$	$\alpha > 0, \beta > 0$
Generalized Extreme Value	$f(x) = \frac{1}{\sigma} t(x)^{\xi+1} e^{-t(x)}$	$t(x) = \begin{cases} \left(1 + \xi \left(\frac{x - \mu}{\sigma}\right)\right)^{-\frac{1}{\xi}} & \text{if } \xi \neq 0 \\ e^{-\frac{(x - \mu)}{\sigma}} & \text{if } \xi = 0 \end{cases}$ $\mu \in \text{Location}$ $\sigma \geq 0 = \text{Scale}$ $\xi \in \text{Shape}$
Burr	$f(x) = \frac{cd}{bz^{c+1} (1 + z^{-c})^{d-1}}$	$\text{where } z = \left(\frac{x - a}{b}\right)$ $a > x, b > 0, c > 0, d > 0$

2-6. Evaluation Criteria

Evaluation of the performance of two evaporation pans should be calculated by several criteria (Naderpour et al., 2018; Ghazvinian et al., 2019). In the present study, according to Equations 3 to 5, the criteria of the Mean Absolute Error (MAE) (Karami et al., 2021), Root Mean Square Error (RMSE) (Ghazvinian et al., 2020a) and coefficient of determination (R^2) were used for the evaluation of the results. The closer the R^2 index is to one, the greater the correspondence is between the data of the two pans (Ferdowsi et al., 2021). The MAE and RMSE indices also show the test error rate, so the closer they are to zero, the more accurate the data matching (Khademi et al., 2021).

$$MAE = \frac{1}{n} \sum_{i=1}^n |E_{ClassA} - E_{Colorado}| \quad (3)$$

$$RMSE = \sqrt{\frac{1}{n} \sum_{i=1}^n (E_{ClassA} - E_{Colorado})^2} \quad (4)$$

$$R^2 = \left[\frac{\sum_{i=1}^n (E_{ClassA} - \bar{E}_{ClassA})(E_{Colorado} - \bar{E}_{Colorado})}{\sqrt{\sum_{i=1}^n (E_{ClassA} - \bar{E}_{ClassA})^2 \sum_{i=1}^n (E_{Colorado} - \bar{E}_{Colorado})^2}} \right]^2 \quad (5)$$

3. Results and Discussion:

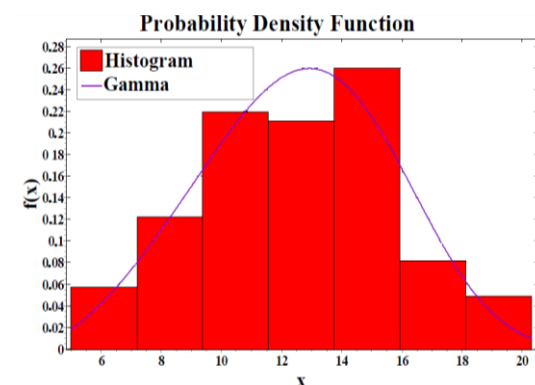
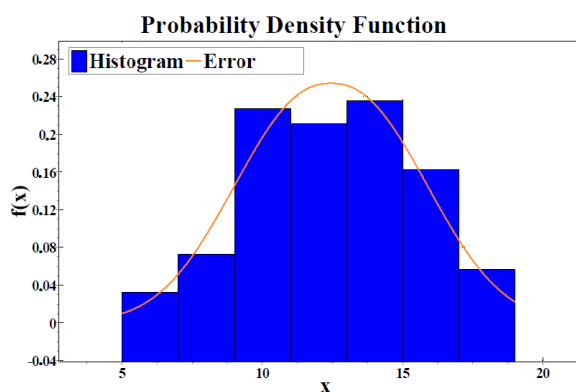
3-1. Statistical results

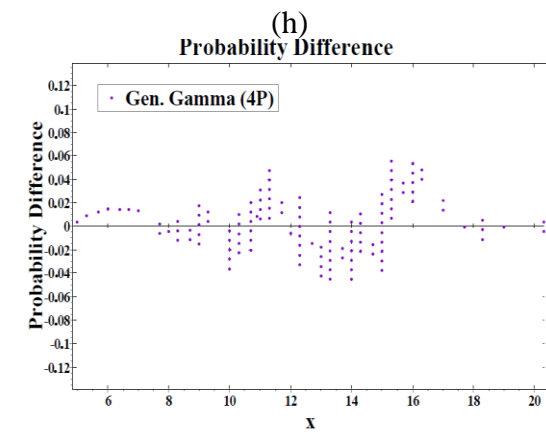
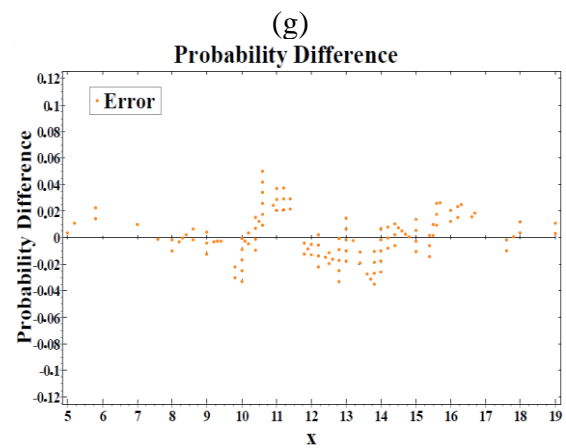
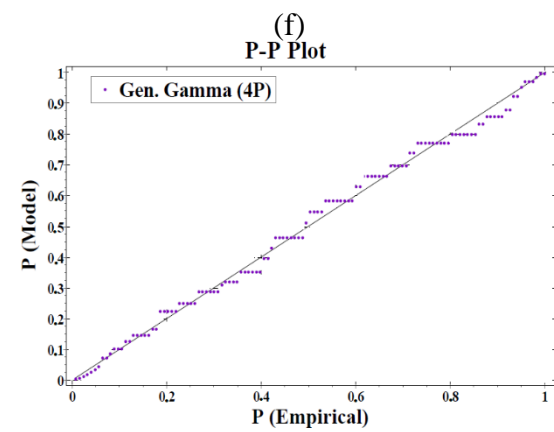
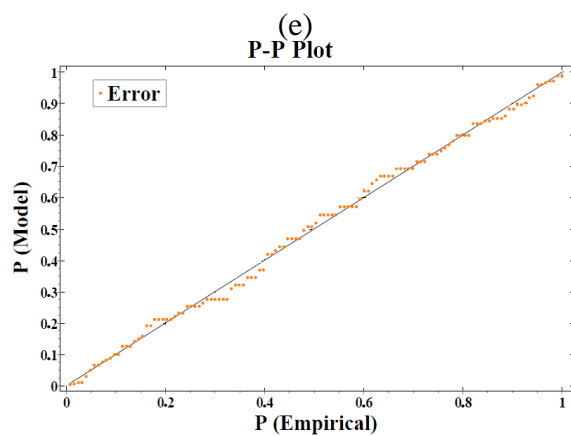
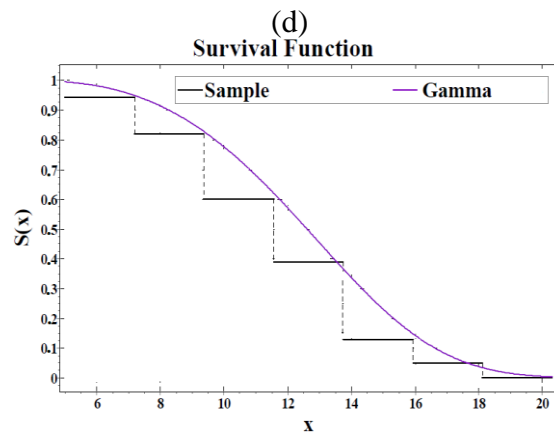
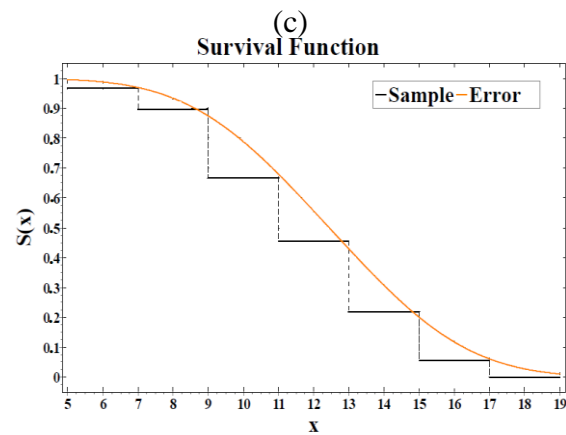
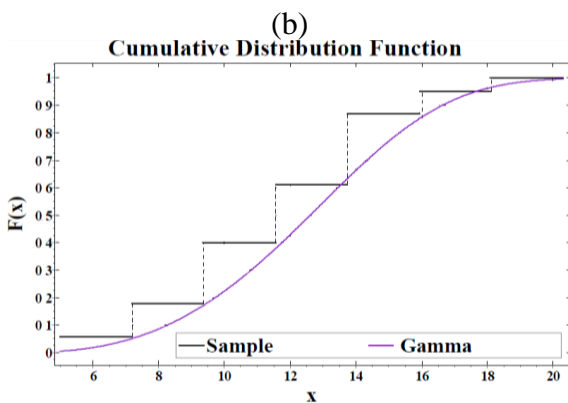
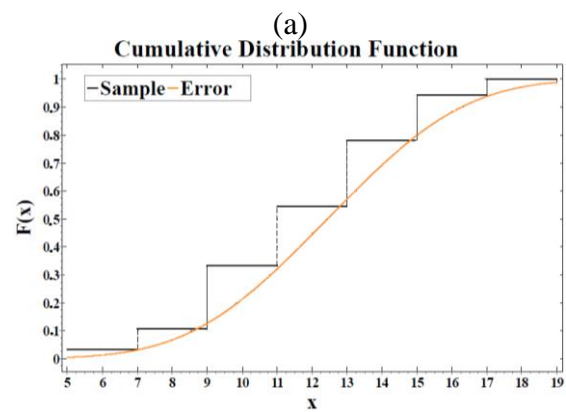
Table 3 shows the results of the statistical analysis of the evaporation of CASEP and CSSEP in millimeters. As can be seen, the average evaporation height of CASEP and the observed evaporation height of CSSEP are close to each other.

Table 3: Results of Statistical Analysis of Evaporation Height of CASEP and CSSEP in millimeters.

Pan	Mean	Standard Error	Median	Mode	Standard deviation	Variance	Kurtosis	Skewness	Number
CSAEP	12.4	0.26	12.60	10.6	2.95	8.71	-0.24	-0.14	123
CSSEP	12.55	0.28	13.00	15.0	3.17	10.07	-0.20	-0.10	123

Statistical analysis of the evaporation data of the CASEP and CSSEP shows that there was not a significant difference between CASEP and CSSEP for the four time periods, May 22 to June 21, June 22 to July 22, July 23 to August 22, and August 23 to September 22. It also shows that there was not a significant difference between the results of two pans for the total daily evaporation data ($P \geq 0.05$). Table 4 shows the statistical analysis of CSSEP and CASEP evaporation using the t-test method for these four time periods tested and the total data. The reason for the lack of significant differences between the data of the two pans may be due to the proximity of the location of the two pans to each other, which would collect the same meteorological data such as daily average air temperature, average daily relative humidity, average daily wind speed, sunlight hours and air pressure. Table 5 shows the results of the statistical distribution fitting test for evaporation from the CASEP and CSSEP at the synoptic station of Semnan. In Table 5, the top five distributions based on the Kolmogorov-Smirnov test for each of the two pans are shown. The Error and Gamma distributions were the best for CASEP and CSSEP, respectively. Figure 6 shows the Probability Density Function, Cumulative Distribution Function, Survival Function, P-P Plot, Q-Q Plot, and Probability Difference diagrams for superior distribution in CASEP and CSSEP.





(i)

(j)

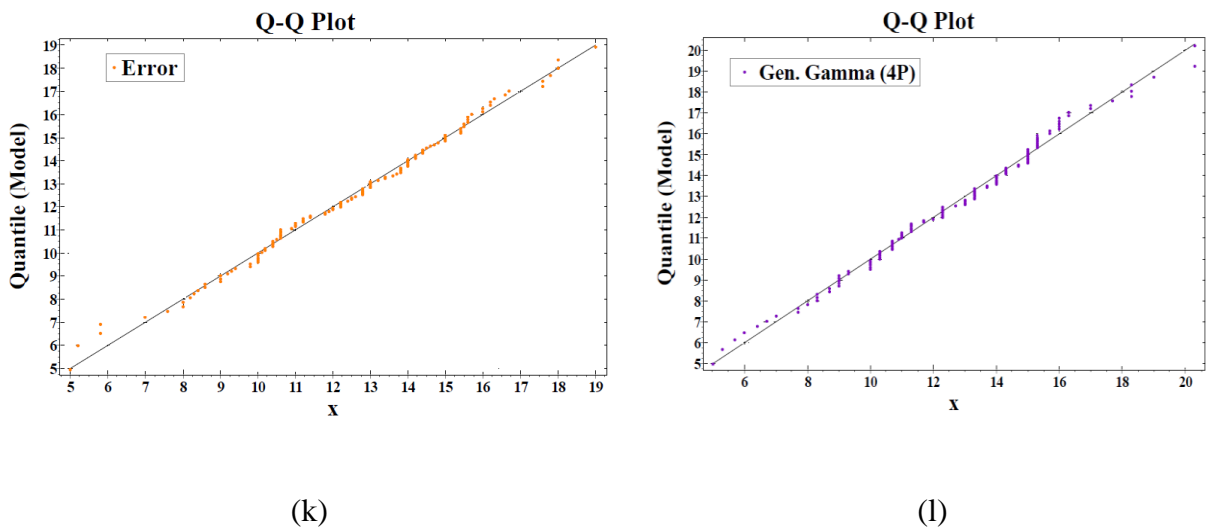


Figure 6: Prediction with selected daily evaporation distributions of the Semnan station for CASEP and CSSEP, respectively, a and b: Probability Density Function diagram, c and d: Cumulative Distribution Function diagram, e and f: Survival Function, g and h: P-P Plot, I and j: Probability Difference, k and l: Q-Q plot.

Table 4: Output of statistical analysis of the CSSEP and CASEP evaporation by the t-test method.

Period	<i>t</i> -Statistic	<i>df</i>	<i>p</i> -Value
22May to 21June	0.3	58	0.7678
22June to 22July	-0.88	60	0.3841
23July to 22Aguest	-0.57	60	0.5719
23Aguest to 22September	0.18	60	0.8556
Total	-0.26	244	0.7918

Table 5: Superior distributions of evaporation data of the studied pans.

Pan name	Rank	Distribution	k-s
CASEP	1	Error	0.05019
	2	Pearson 6	0.05286
	3	Log normal	0.0538
	4	Weibull	0.0539
	5	Kumaraswamy	0.05431
CSSEP	1	Gamma	0.05552
	2	Kumaraswamy	0.05776
	3	Weibull	0.05807
	4	Burr	0.05829
	5	Generalized Extreme Value	0.05852

3.2. Results of Evaporation Values of CASEP and CSSEP

Figure 7 shows the average ER of the CASEP and CSSEP for four different time periods. In general, this diagram shows that the results of the two pans are close to each other and their difference is less than 1 mm. In the first period, from May 22 to June 21, and in the fourth period, from August 23 to September 22, the ER of the CSSEP was lower than that of the CASEP, and in the second and third periods, from 22 June to July 22, and July 23 to August 22, the ER of the CSSEP is higher than that of the CASEP, respectively.

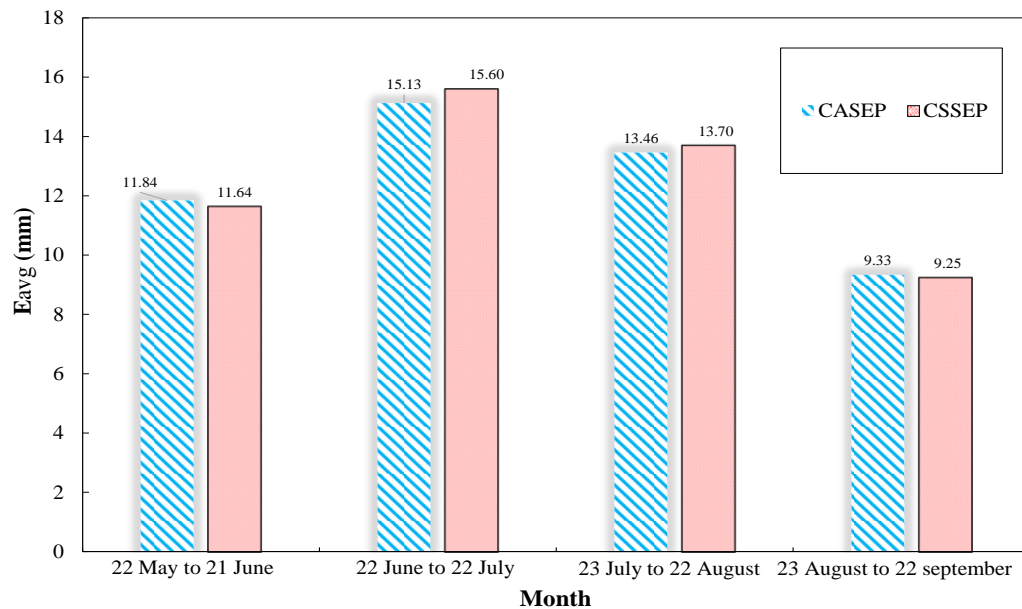


Figure 7: Comparison of the average ER of the CASEP and CSSEP for four time periods.

Figure 8 compares the ER in the CASEP and CSSEP, on all measured days. This diagram shows that the maximum ER in both pans is during the period approximately from the 30th to the 70th day. Also, during the measurement days, on some of these days, the ER of the CASEP is higher than the ER of the CSSEP and on some days the CASEP is lower than the ER of the CSSEP. The results from Masoner et al. (2008) showed that the difference between the ER in a floating pan and the evaporation pan of class A on the ground at night is less than during the day. In general, the results of this study showed that the floating evaporation pan in the free surface of water can be better in determining the ER. The similarity ratio of a floating pan with a pan placed on the ground varies during the measurement period and varies from 0.69 to 0.87.

Chu et al. (2016) who compared two CASEPs, one painted galvanized and the other white, concluded that the ER of the white pan was lower in all months of measurement. The average annual evaporation values in galvanized and white sheet pans were 1.392 and 1.041, respectively.

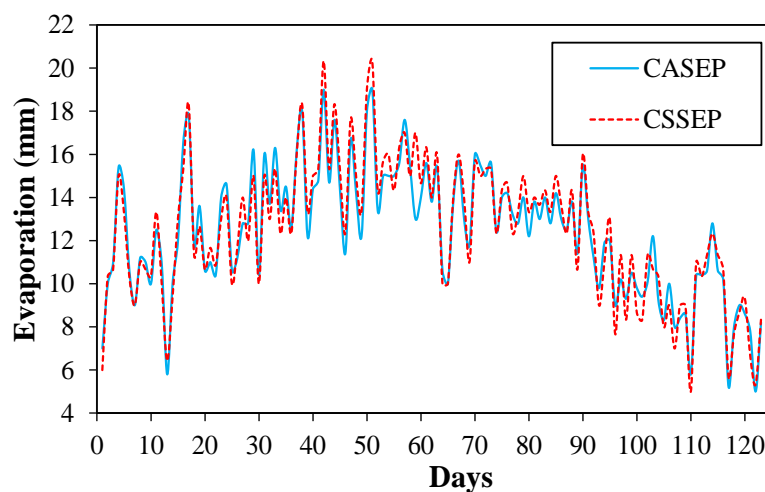


Figure 8: Comparison of daily evaporation of the CSSEP and CASEP.

Figure 9 shows the cumulative diagram ER of the CASEP and CSSEP. Figure 9, like Figure 8, shows the approximate daily ER in the two studied pans. The diagram also shows that the ER in the CSSEP at the end of the experiment is slightly higher than the ER in the CASEP.

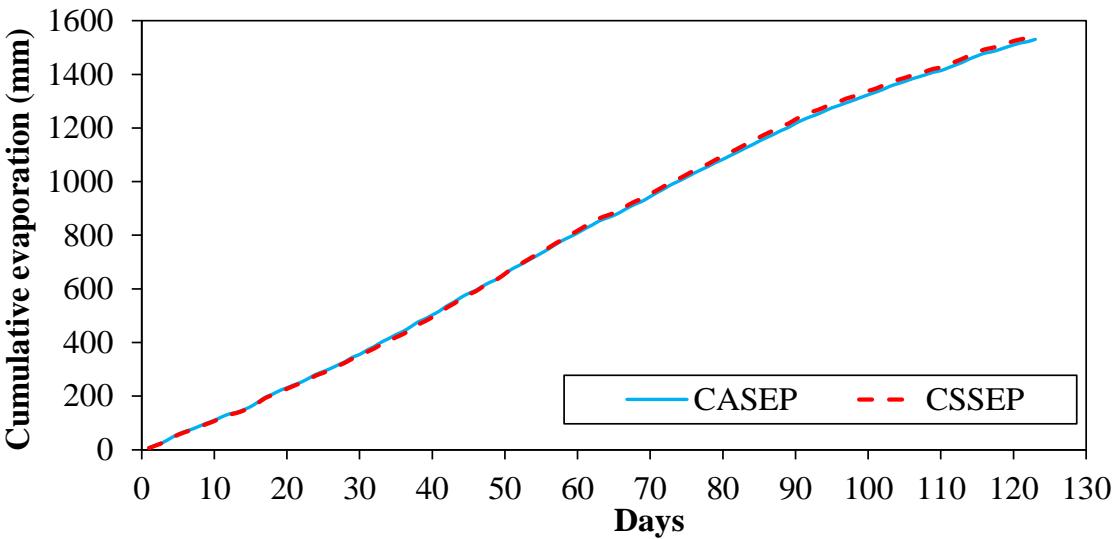


Figure 9: Comparison of cumulative evaporation of the CASEP and CSSEP.

3.3. Investigation of parameters

In order to correlate the evaporation of the CASEP and CSSEP with the station data, which includes minimum temperature (C), maximum temperature (C), minimum humidity (%), maximum humidity (%), wind speed (m / s), sunlight hours (hr) and pressure (hPa), the Pearson correlation test was used. Table 4 shows the mean and standard deviation of meteorological parameters. Table 5 shows the correlation of evaporation of the pans with minimum and maximum temperature, minimum and maximum humidity, wind speed, pressure and hours of sunlight. In other words, evaporation increases if the temperature and sunlight hours increase. The correlation between evaporation and wind speed is positive. However, the wind parameter, with the evaporation of the pans, is not significant, as it has no effect on the process of evaporation of the pans. Also in Table 5, the correlations of minimum humidity, maximum humidity, and pressure are negative. This indicates that evaporation decreases if humidity and pressure increase. It should be noted that all parameters, except wind speed, are at a significance level of less than 5%.

Table 4: Mean and standard deviation of meteorological parameters affecting evaporation.

	PA(hpa)	SH(hr)	WS(m/s)	RH _{min} (%)	RH _{max} (%)	T _{min} (c)	T _{max} (c)
Number	123	123	123	123	123	123	123
Mean	884.110	11.191	7.553	11.106	28.992	25.037	37.052
Standard deviation	9.8758	1.5495	2.4199	5.2679	9.9568	3.4044	3.3354

Table 5: Pearson correlation test and significance level of data for the CASEP and CSSEP.

		PA(hpa)	SH(hr)	WS(m/s)	RH _{min} (%)	RH _{max} (%)	T _{min} (c)	T _{max} (c)
CASEP	Pearson correlation	-0.221	0.369	0.158	-0.314	-0.303	0.513	0.623
	Two sided Sig	0.014	0.000	0.0081	0.000	0.001	0.000	0.000
	number	123	123	123	123	123	123	123

CSSEP	Pearson correlation	-0.233	0.399	0.126	-0.320	-0.336	-.0552	0.647
	Two sided Sig	0.010	0.000	0.166	0.000	0.000	0.000	0.000
	number	123	123	123	123	123	123	123

Figure 10 compares the changes of the parameters received from Semnan meteorological station including minimum temperature (Celsius), maximum temperature (Celsius), maximum humidity (percentage), minimum humidity (percentage), sunlight hours, pressure (hectopascal) and wind speed (meters per second) on test days; it also shows the rate of evaporation from the CASEP and CSSEP (mm) (Ghazvinian et al., 2021). From the obtained results, it can be deduced that wind speed and temperature are at their lowest correlation with the ER. Therefore, comparing the results of these two parameters with other parameters, it can be assumed that wind speed at a height of 2 meters above the ground has the least effect on evaporation.

3-4. Results of evaluation criteria

Statistical indices related to the fitting of the evaporation data of CASEP and CSSEP shows that there is a high correlation between the data of these two pans. Estimates are made for the whole data. The values of R², RMSE and MAE are 0.933, 0.835 and 0.702, respectively.

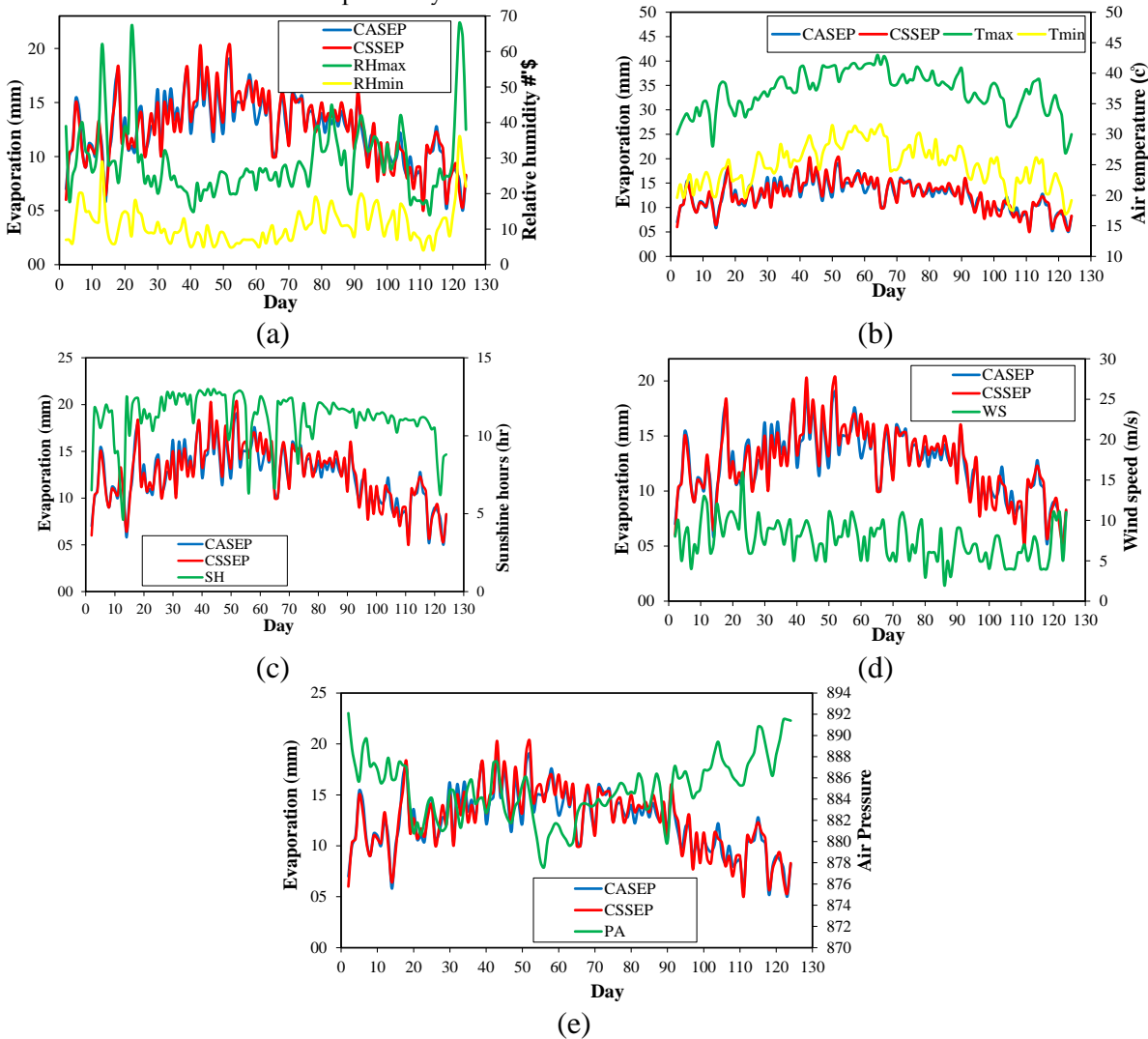


Figure 10: Comparison of changes in the CASEP and CSSEP with meteorological parameters, a) minimum and maximum relative humidity, b) minimum and maximum temperature, c) sunlight hours, d) wind speed and e) air pressure.

Taylor diagrams were plotted to investigate the values of standard deviation, correlation coefficient, and root mean square error between the CASEP and CSSEP data (Figure 11). It should be noted that in the Taylor diagram, the longitudinal distance from the origin of the coordinates represents the correlation coefficient and the segmental lines represent the square root values of the mean squares of the error. As the circle segment increases, the value of this parameter increases. In other words, each point on the Taylor diagram represents, simultaneously, three parameters of standard deviation, correlation coefficient, and the root mean square error (Taylor, 2001).

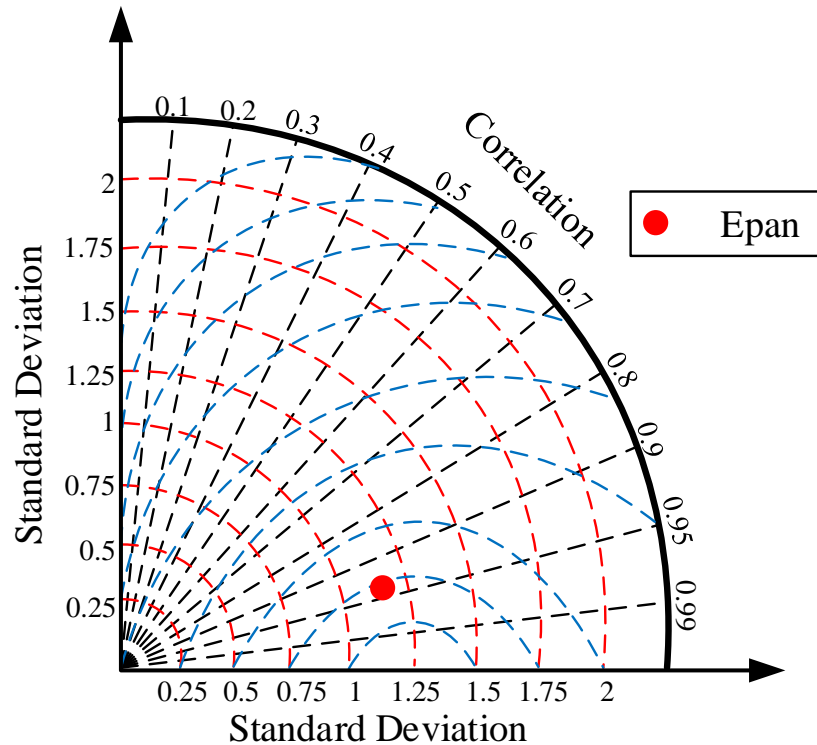


Figure 11: Taylor diagram between the CASEP and CSSEP.

4-. Conclusion

In this paper, the daily evaporation of Semnan city was measured for 123 days (4 months) in the CSSEP and then compared with the CASEP of the synoptic station of Semnan city. Due to the fact that the city of Semnan is one of the hottest and driest areas in the region, the test days were from the end of spring through the entire summer, when evaporation is highest. In this study, the relationship between the evaporation of the pan with the meteorological data of Semnan Synoptic Station was investigated. There is no significant difference between the CSSEP and CASEP and the coefficient of determination between the amounts of evaporation in two pans is equal to 93.3%, which shows a high correlation between evaporation of pans. The best statistical distributions based on the Klomogorov-Sminrov method for the CASEP and CSSEP were Error and Gamma, respectively. Minimum temperature, maximum temperature and sunlight data have a significant positive correlation with the CSSEP and CASEP pans and minimum humidity, maximum humidity and pressure have a significant negative correlation with these two pans. Also, wind speed data in the CSSEP and CASEP showed a significant lack of correlation. This can be due to the constant and relatively low wind speed during the test period. The highest correlation is with the minimum temperature and the lowest is with pressure. Finally, we suggest studying the effect of wind during cold seasons on evaporation pans in hot and dry areas.

References

- Alsumaiei, A. A. (2020). Utility of Artificial Neural Networks in Modeling Pan Evaporation in Hyper-Arid Climates. *Water* 12, 1508. doi:10.3390/w12051508.
- Ashrafzadeh, A., Malik, A., Jothiprakash, V., Ghorbani, M. A., and Biazar, S. M. (2020). Estimation of daily pan evaporation using neural networks and meta-heuristic approaches. *ISH J. Hydraul. Eng.* 26, 421–429. doi:10.1080/09715010.2018.1498754.
- Brunner, G. W., and Fleming, M. J. (2010). HEC-SSP Statistical Software Package. *US Army Corps Eng. Inst. Water Resour. Hydrol. Eng. Cent. HEC. Available* <https://www.hec.usace.army.mil/software/hec-ssp>.
- Brutsaert, W. (1982). *Evaporation into the Atmosphere*. Dordrecht: Springer Netherlands doi:10.1007/978-94-017-1497-6.
- Chu, C.-R., Li, M.-H., Chen, C.-H., and Liu, J.-S. (2016). Evaporation Rate of a White Class A Evaporation Pan. *J. Irrig. Drain. Eng.* 142, 04016018. doi:10.1061/(ASCE)IR.1943-4774.0001026.
- Chu, C.-R., Li, M.-H., Chen, Y.-Y., and Kuo, Y.-H. (2010). A wind tunnel experiment on the evaporation rate of Class A evaporation pan. *J. Hydrol.* 381, 221–224. doi:10.1016/j.jhydrol.2009.11.044.
- Dehghanipour, M. H., Karami, H., Ghazvinian, H., Kalantari, Z., and Dehghanipour, A. H. (2021). Two Comprehensive and Practical Methods for Simulating Pan Evaporation under Different Climatic Conditions in Iran. *Water* 13, 2814. doi:10.3390/w13202814.
- Ferdowsi, A., Nemati, M., and Farzin, S. (2021). Development of Dam-Break Model Considering Real Case Studies with Asymmetric Reservoirs. *Comput. Eng. Phys. Model.* 4, 39–63. doi:10.22115/cepm.2021.311759.1188.
- Fu, G., Liu, C., Chen, S., and Hong, J. (2004). Investigating the conversion coefficients for free water surface evaporation of different evaporation pans. *Hydrol. Process.* 18, 2247–2262. doi:10.1002/hyp.5526.
- Ghazvinian, H., Bahrami, H., Ghazvinian, H., and Heddami, S. (2020a). Simulation of Monthly Precipitation in Semnan City Using ANN Artificial Intelligence Model. *J. Soft Comput. Civ. Eng.* 4, 36–46. doi:10.22115/scce.2020.242813.1251.
- Ghazvinian, H., Farzin, S., Karami, H., and Mousavi, S. F. (2020b). Investigating the Effect of using Polystyrene sheets on Evaporation Reduction from Water-storage Reservoirs in Arid and Semi-arid Regions (Case study: Semnan city). *J. Water Sustain. Dev.* 7, 45–52. doi:10.22067/jwsd.v7i2.81748.
- Ghazvinian, H., Karami, H., Farzin, S., and Mousavi, S.-F. (2021). Introducing affordable and accessible physical covers to reduce evaporation from agricultural water reservoirs and pools (field study, statistics, and intelligent methods). *Arab. J. Geosci.* 14, 2543. doi:10.1007/s12517-021-08735-3.
- Ghazvinian, H., Karami, H., Farzin, S., and Mousavi, S. F. (2020c). Effect of MDF-Cover for Water Reservoir Evaporation Reduction, Experimental, and Soft Computing Approaches. *J. Soft Comput. Civ. Eng.* 4, 98–110. doi:10.22115/scce.2020.213617.1156.
- Ghazvinian, H., Karami, H., Farzin, S., and Mousavi, S. F. (2020d). Experimental Study of Evaporation Reduction Using Polystyrene Coating, Wood and Wax and its Estimation by Intelligent Algorithms. *Irrig. Water Eng.* 11, 147–165. doi:10.22125/iwe.2020.120727.
- Ghazvinian, H., Mousavi, S.-F., Karami, H., Farzin, S., Ehteram, M., Hossain, M. S., et al. (2019). Integrated support vector regression and an improved particle swarm optimization-based model for solar radiation prediction. *PLoS One* 14, e0217634. doi:10.1371/journal.pone.0217634.
- Ghorbani, K., Aligholnia, T., and Rasouli Majd, N. (2018). Accuracy Evaluation of Twenty Empirical Models in Estimating Coastal Regions Reference Evapotranspiration in different climate. *J. Water Soil Conserv.* 25, 307–320. doi:10.22069/jwsc.2018.14411.2917.
- Güven, A., and Kışi, Ö. (2011). Daily pan evaporation modeling using linear genetic programming technique. *Irrig. Sci.* 29, 135–145. doi:10.1007/s00271-010-0225-5.
- Harris, J., Brunner, G., and Faber, B. (2008). Statistical Software Package. in *World Environmental and Water Resources Congress 2008* (Reston, VA: American Society of Civil Engineers), 1–10. doi:10.1061/40976(316)568.
- Jahan, F., Sinha, N. C., Rahman, M. M., Rahman, M. M., Mondal, M. S. H., and Islam, M. A. (2019). Comparison of missing value estimation techniques in rainfall data of Bangladesh. *Theor. Appl. Climatol.* 136, 1115–1131. doi:10.1007/s00704-018-2537-y.
- Jia-lian, H., Guo-bin, F. U., Zao-nan, G. U. O., Zhande, D., and Wei, Z. (1996). Experimental research on the water-surface evaporation of Nansi Lake in Shandong Province. *Geogr. Res.* 15, 42–49.
- Jia, Z., Liu, S., Xu, Z., Chen, Y., and Zhu, M. (2012). Validation of remotely sensed evapotranspiration over the Hai River Basin, China. *J. Geophys. Res. Atmos.* 117, n/a-n/a. doi:10.1029/2011JD017037.
- Karami, H., Ghazvinian, H., Dehghanipour, M., and Ferdosian, M. (2021). Investigating the Performance of Neural Network Based Group Method of Data Handling to Pan's Daily Evaporation Estimation (Case Study: Garmsar City). *J. Soft Comput. Civ. Eng.*, 1–18. doi:10.22115/scce.2021.274484.1282.

- Karamouz, M., Nazif, S., and Falahi, M. (2012). *Hydrology and hydroclimatology: principles and applications*. 6000 Broken Sound Parkway NW, Suite 300: CRC Press.
- Khademi, A., Behfarnia, K., Kalman Šipoš, T., and Miličević, I. (2021). The Use of Machine Learning Models in Estimating the Compressive Strength of Recycled Brick Aggregate Concrete. *Comput. Eng. Phys. Model.* 4, 1–25. doi:10.22115/cepm.2021.297016.1181.
- Kohler, M. A. (1954). Lake and pan evaporation. *Water-Loss Investig. Lake Hefner Stud. Tech. Report, United States Geol. Surv. Prof. Pap.* 269, 127–149.
- Li, Y., Liu, C., and Liang, K. (2016). Spatial Patterns and Influence Factors of Conversion Coefficients between Two Typical Pan Evaporimeters in China. *Water* 8, 422. doi:10.3390/w8100422.
- Liu, B., Ma, Z., Xu, J., and Xiao, Z. (2009). Comparison of pan evaporation and actual evaporation estimated by land surface model in Xinjiang from 1960 to 2005. *J. Geogr. Sci.* 19, 502–512. doi:10.1007/s11442-009-0502-5.
- Malik, A., and Kumar, A. (2015). Pan Evaporation Simulation Based on Daily Meteorological Data Using Soft Computing Techniques and Multiple Linear Regression. *Water Resour. Manag.* 29, 1859–1872. doi:10.1007/s11269-015-0915-0.
- Masoner, J. R., Stannard, D. I., and Christenson, S. C. (2008). Differences in Evaporation Between a Floating Pan and Class A Pan on Land. *J. Am. Water Resour. Assoc.* 44, 552–561. doi:10.1111/j.1752-1688.2008.00181.x.
- Massey Jr, F. J. (1951). The Kolmogorov-Smirnov test for goodness of fit. *J. Am. Stat. Assoc.* 46, 68–78.
- McMahon, T. A., Peel, M. C., Lowe, L., Srikanthan, R., and McVicar, T. R. (2013). Estimating actual, potential, reference crop and pan evaporation using standard meteorological data: a pragmatic synthesis. *Hydrol. Earth Syst. Sci.* 17, 1331–1363. doi:10.5194/hess-17-1331-2013.
- Miralles, D. G., Jiménez, C., Jung, M., Michel, D., Ershadi, A., McCabe, M. F., et al. (2015). The WACMOS-ET project – Part 2: Evaluation of global terrestrial evaporation data sets. *Hydrol. Earth Syst. Sci. Discuss.* 12, 10651–10700. doi:10.5194/hessd-12-10651-2015.
- Moghaddamnia, A., Ghafari Gousheh, M., Piri, J., Amin, S., and Han, D. (2009). Evaporation estimation using artificial neural networks and adaptive neuro-fuzzy inference system techniques. *Adv. Water Resour.* 32, 88–97. doi:10.1016/j.advwatres.2008.10.005.
- Naderpour, H., Rafiean, A. H., and Fakharian, P. (2018). Compressive strength prediction of environmentally friendly concrete using artificial neural networks. *J. Build. Eng.* 16, 213–219. doi:10.1016/j.jobbe.2018.01.007.
- Nourani, V., and Sayyah Fard, M. (2012). Sensitivity analysis of the artificial neural network outputs in simulation of the evaporation process at different climatologic regimes. *Adv. Eng. Softw.* 47, 127–146. doi:10.1016/j.advengsoft.2011.12.014.
- Patle, G. T., Chettri, M., and Jhajharia, D. (2020). Monthly pan evaporation modelling using multiple linear regression and artificial neural network techniques. *Water Supply* 20, 800–808. doi:10.2166/ws.2019.189.
- Piri, J., Amin, S., Moghaddamnia, A., Keshavarz, A., Han, D., and Remesan, R. (2009). Daily Pan Evaporation Modeling in a Hot and Dry Climate. *J. Hydrol. Eng.* 14, 803–811. doi:10.1061/(ASCE)HE.1943-5584.0000056.
- Root, K., and Papakos, T. H. (2010). Hydrologic Analysis of Flash Floods in Sana'a, Yemen. in *Watershed Management 2010* (Reston, VA: American Society of Civil Engineers), 1248–1259. doi:10.1061/41143(394)112.
- Simba, F. M., and Matorevhu, A. (2013). Exploring Estimation of Evaporation in Dry Climates Using a Class ?A? Evaporation Pan. *Irrig. Drain. Syst. Eng.* 2. doi:10.4172/2168-9768.1000109.
- Simolo, C., Brunetti, M., Maugeri, M., and Nanni, T. (2010). Improving estimation of missing values in daily precipitation series by a probability density function-preserving approach. *Int. J. Climatol.* 30, 1564–1576.
- Stanhill, G. (2002). Is the Class A evaporation pan still the most practical and accurate meteorological method for determining irrigation water requirements? *Agric. For. Meteorol.* 112, 233–236. doi:10.1016/S0168-1923(02)00132-6.
- Subramanya, K. (2013). *Engineering hydrology, 4e*. Tata McGraw-Hill Education.
- Taylor, K. E. (2001). Summarizing multiple aspects of model performance in a single diagram. *J. Geophys. Res. Atmos.* 106, 7183–7192. doi:10.1029/2000JD900719.
- Torres, E. A., and Calera, A. (2010). Bare soil evaporation under high evaporation demand: a proposed modification to the FAO-56 model. *Hydrol. Sci. J.* 55, 303–315. doi:10.1080/02626661003683249.
- Traore, S., Luo, Y., and Fipps, G. (2016). Deployment of artificial neural network for short-term forecasting of evapotranspiration using public weather forecast restricted messages. *Agric. Water Manag.* 163, 363–379. doi:10.1016/j.agwat.2015.10.009.
- Traore, S., Wang, Y.-M., and Kerh, T. (2010). Artificial neural network for modeling reference evapotranspiration complex process in Sudano-Sahelian zone. *Agric. Water Manag.* 97, 707–714. doi:10.1016/j.agwat.2010.01.002.
- Wang, L., Niu, Z., Kisi, O., Li, C., and Yu, D. (2017). Pan evaporation modeling using four different heuristic approaches. *Comput. Electron. Agric.* 140, 203–213. doi:10.1016/j.compag.2017.05.036.

- Wilks, D. S. (1995). Statistical methods in the Atmospheric Sciences, 1995. *Libr. Cat. Acad. Press San Diego, CA*, 465.
- Wurbs, R. A., and Ayala, R. A. (2014). Reservoir evaporation in Texas, USA. *J. Hydrol.* 510, 1–9. doi:10.1016/j.jhydrol.2013.12.011.